Supplement of Atmos. Meas. Tech., 18, 4227–4247, 2025
https://doi.org/10.5194/amt-18-4227-2025-supplement

Atmospheric Measurement Techniques
Open Access

Supplement of

Identifying key parameters that affect sensitivity of flow tube chemical ionization mass spectrometers

Sneha Aggarwal et al.

Correspondence to: Claudia Mohr (claudia.mohr@psi.ch) and Felipe Lopez-Hilfiker (lopez@tofwerk.com)

Supplemental Information

Model	IMR (V)	Q1 front and back (V)	RF–only Q (V)	Skimmer (V)	Q2 front (V)	Q2 back(V)	Skimmer 2 (V)	IMR (mbar)	SQ (mbar)	BSQ (mbar)	Resolving Power (M/dM)
Tofwerk Vocus B	0	0	100	1	2	3	5	50	1.5	10^{-2}	1200
Tofwerk Vocus B2	0	0	100	1	2	3	5	50	1.5	10^{-2}	5000
Tofwerk Vocus B4	0	0	100	1	2	3	5	50	1.5	10^{-2}	10000
Tofwerk Vocus 2R	0	0	100	1	2	3	5	50	2	10^{-2}	10000
Tofwerk Vocus S	0	0	100	1	2	3	5	50	2	10^{-2}	5000
Tofwerk Vocus Scout	0	0	100	1	2	3	5	50	2	10^{-2}	3500

Table S1. Typical voltage settings and effective pressure across the different interfaces for the different instruments used in this study. The voltages in the above table correspond to negative ion mode, the polarity of the Skimmer, Q2 Front, Q2 Back, and Skimmer 2 are inverted for positive ion mode.

Compound	Reagent Ion	Sensitivity (ncps ppt^{-1})	Proton Affinity (kcal mol^{-1})	Ionization Energy (eV)	Chemical Formula
Xylene	Benzene (+)	10	188.0 ± 1.11 (Chong and Franklin, 1971)	8.44 ± 0.05 (NIST WebBook)	C_8H_{10}
Trimethylbenzene (TMB)	Benzene (+)	11	199.85 (NIST WebBook)	8.4 ± 0.01 (NIST WebBook)	C_9H_{12}
α–pinene	Benzene (+)	12	206.3 (Canaval et al., 2019)	8.07 (NIST WebBook)	$C_{10}H_{16}$
Levoglucosan	Iodide (–)	8.3	192.13 (Rocha et al., 2013)	8.78 (Rocha et al., 2013)	$C_6H_{10}O_5$
PFPeA	Iodide (–)	10.4	N/A	N/A	$C_5HF_9O_2$
PFBA	Iodide (–)	10.3	N/A	N/A	$C_4HF_7O_2$
Chlorine	Bromide (–)	12.5	131.40 (Cacace et al., 1998)	11.48 ± 0.003 (NIST WebBook)	Cl_2
Levoglucosan	Bromide (–)	10.5	192.13 (Rocha et al., 2013)	8.78 (Rocha et al., 2013)	$C_6H_{10}O_5$
Dimethylaniline	Acetone (+)	8.5	224.93 (NIST WebBook)	7.12 ± 0.02 (NIST WebBook)	$C_8H_{11}N$
Ethanolamine	Acetone (+)	8.1	222.33 (NIST WebBook)	8.96 (NIST WebBook)	C_2H_7NO
PGMEA	Acetone (+)	12.4	N/A	N/A	$C_6H_{12}O_3$
Diethylamine	Ethanol (+)	9.5	222.15583	8.2 ± 0.1	$C_4H_{11}N$
PFHxA	Nitrate (–)	8.7	N/A	N/A	$C_6HF_{11}O_2$

Table S2. Compounds and sensitivities used to quantify the collision-limited sensitivity for different reagent ions presented in Figure 7. (PFPeA: perfluoropentanoic acid; PFBA: perfluorobutanoic acid; PGMEA: propylene glycol monomethyl ether acetate)

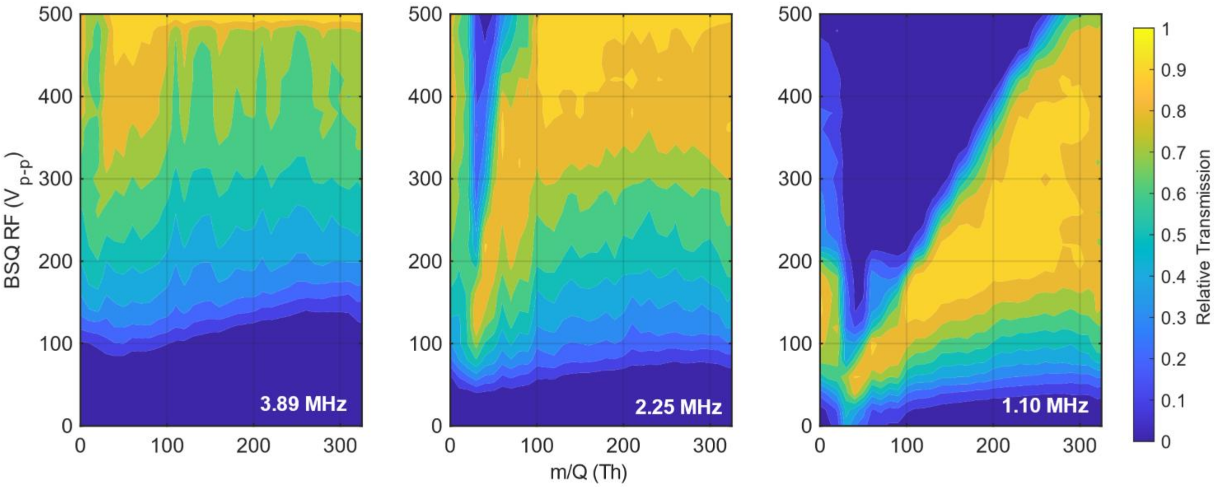

Figure S1. Radio frequency (RF) amplitudes (peak–to–peak Voltage, $V_{p\text{–}p}$) at different resonant frequencies and the relative transmission efficiency as a function of mass normalized to the global maximum transmission across all panels in the region of typical reagent ion and analyte compounds This was performed experimentally by scanning the big segmented quadrupole (BSQ) RF amplitude at different resonant frequencies and recording the mass spectrum. Signal intensities increase as a function of the RF amplitude through focusing and are limited by the low mass cut-off of the quadrupole. The relative transmission of the instrument is calculated by taking the maximum signal for each mass bin as a transmission value of 1.0, with all other measurements being relative to this reference. At BSQ RF frequencies of ~4 MHz, the mass discrimination is weakly visible, with overall transmission increasing across the mass range with relatively little bias. At ~2 MHz, the mass discrimination becomes more evident at increased RF amplitudes removing masses less than ~60 Th at RF amplitudes of 300 $V_{p\text{–}p}$ and higher. At lower frequencies the attenuation of lighter masses extends up to 200 Th at the highest RF amplitudes – which poses a significant problem for reagent ion normalization (as the relative transmission across the mass spectrum is not constant).

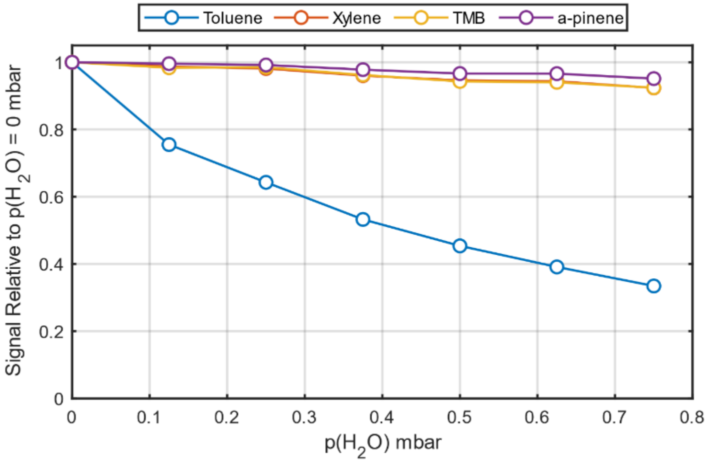

Figure S2. Water vapour dependency for benzene cations as discussed in the text.

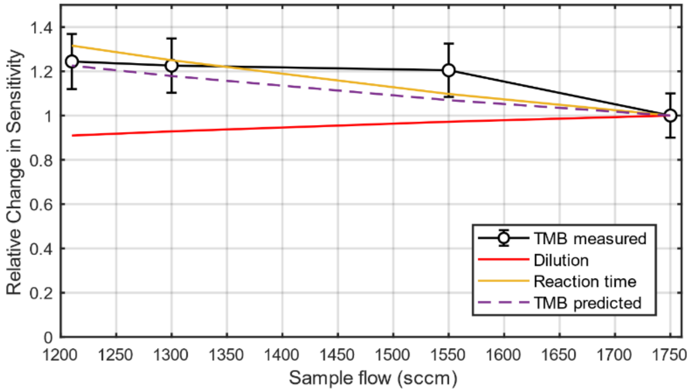

Figure S3. Sensitivity as a function of sample flow, for the example of trimethylbenzene (TMB). Modeled effects of sample dilution and reaction time as well as the net effect on observed sensitivity.

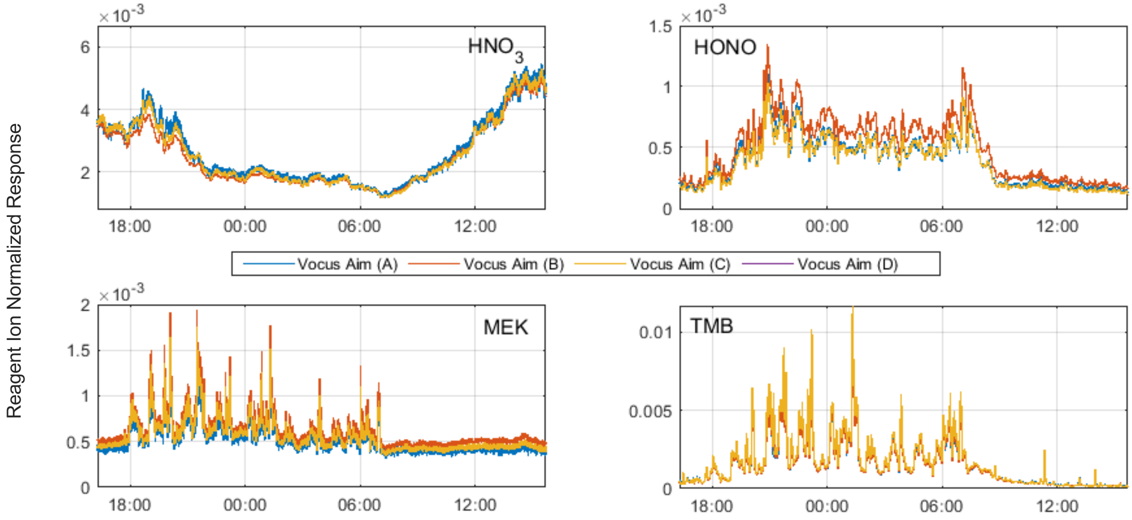

Figure S4. A subset of the data presented in Fig. 6 demonstrating the high frequency correlation and excellent agreement in normalized responses.

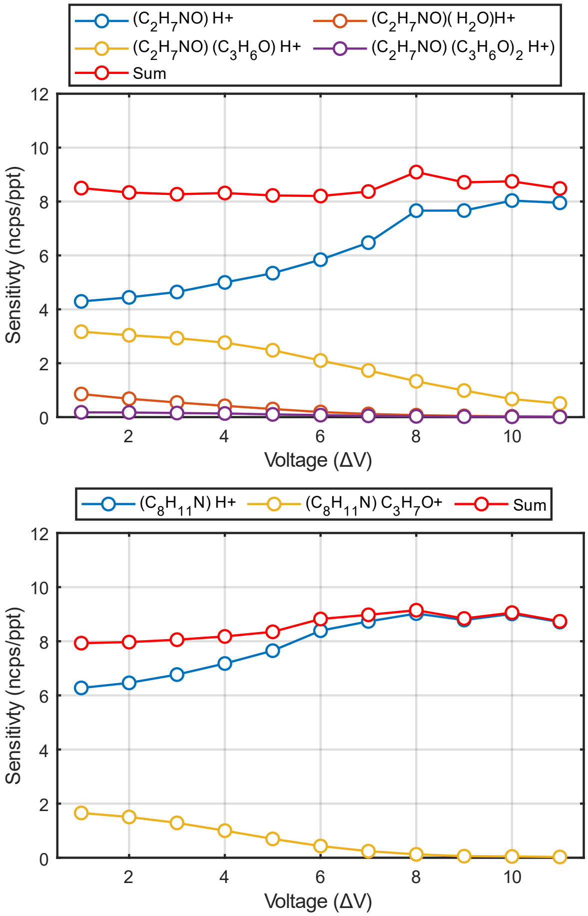

Figure S5. Example of different detection channels for two example amines: ethanolamine (top) and dimethylaniline (below) through reaction with protonated acetone dimers. The sum sensitivity remains constant across the voltage scanning experiment, despite the detection channels shifting as a function of energy. The sum sensitivity is consistent with the collision limited sensitivity within experimental error under each voltage step.

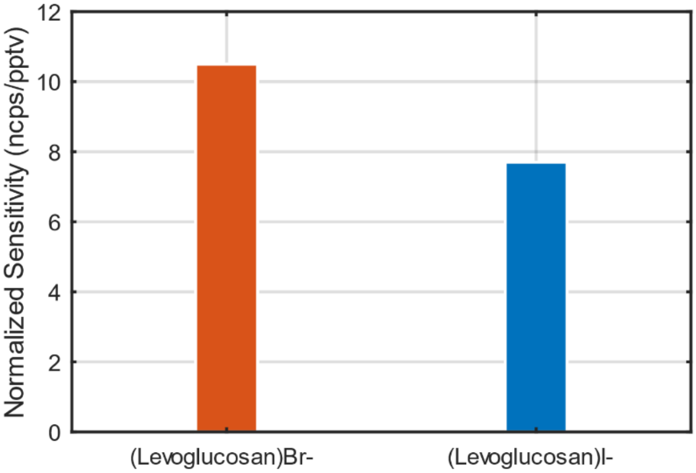

Figure S6. Absolute responses of iodide and bromide adduct reagent ions measuring levoglucosan on the same reactor and instrument simultaneously. The measurements demonstrate that while the assumption that levoglucosan is detected near the collision limit with iodide, it actually is slightly below the collision limit – by roughly 20 % – when compared to bromide. The sensitivity of levoglucosan with Br- anions is consistent with other reagent ions determination of the collision limit within experimental uncertainty.

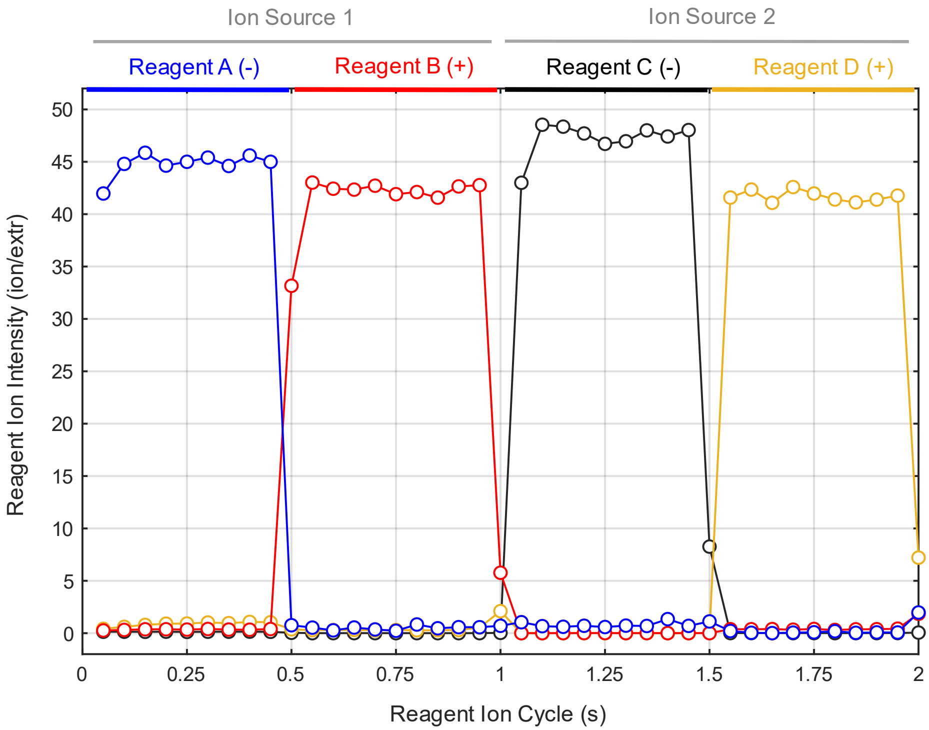

Figure S7. Measurement cycle for fast polarity switching between different reagent ions. Typically, when using 4 reagent ions, the instrument measures for 0.5 s with each reagent ion in a 2-second measurement loop.

References

Cacace, F., de Petris, G., Pepi, F., Rosi, M., and Sgamellotti, A.: Elemental Chlorine and Chlorine Fluoride: Theoretical and Experimental Proton Affinity and the Gas Phase Chemistry of Cl2H + and FClH+ Ions, J. Phys. Chem. A, 102, 10560–10567, https://doi.org/10.1021/jp9831379, 1998.

Canaval, E., Hyttinen, N., Schmidbauer, B., Fischer, L., and Hansel, A.: NH4+ Association and Proton Transfer Reactions with a Series of Organic Molecules, Front Chem, 7, 191, https://doi.org/10.3389/fchem.2019.00191, 2019.

Chong, S.-L. and Franklin, J. L.: Proton affinities of benzene, toulene, and the xylenes, J. Am. Chem. Soc., 94, 6630–6635, https://doi.org/10.1021/ja00774a010, 1972.

Rocha, I. M., Galvão, T. L. P., Sapei, E., Ribeiro da Silva, M. D. M. C., and Ribeiro da Silva, M. A. V.: Levoglucosan: A Calorimetric, Thermodynamic, Spectroscopic, and Computational Investigation, J. Chem. Eng. Data, 58, 1813–1821, https://doi.org/10.1021/je400207t, 2013.